

# Effect of electric fields on solid-state reactions between oxides

## Part 3 *Interdiffusion in polycrystalline magnesium and aluminium oxide pellets*

K. J. D. MACKENZIE, M. J. RYAN

*Chemistry Division, Department of Scientific and Industrial Research, Petone, New Zealand*

Interdiffusion in sintered polycrystalline pellets of MgO and Al<sub>2</sub>O<sub>3</sub> at temperatures in the range 1300 to 1450° C was shown by scanning electron microscope energy dispersive X-ray probe (EDAX) and X-ray diffraction techniques to be enhanced by the application of direct current electric fields, particularly when the alumina pellet is of negative polarity, under which conditions the diffusion activation energy of Mg in Al<sub>2</sub>O<sub>3</sub> is significantly increased. The diffusion process involved, principally, the transport of Mg by grain-boundary diffusion and possibly vapour-phase transport into the interstices of the comparatively porous alumina pellets; only minimal counter-migration of aluminium was observed in these experiments. The Mg-content of the discrete spinel grains within the reaction interface region is increased by electrolysis above the values calculated from solid solubility data, particularly where the alumina pellet is of positive polarity. The excess Mg is most apparent at the side of the spinel grains nearest the reaction interface, and precipitates as a surface MgO layer on the grains. The effective electrical mobility of the migrating species was calculated from the down-field shift of the diffusion profile and compared with values calculated from the electrical conductivity of the system.

### 1. Introduction

In a previous paper [1], it was shown that the extent of solid-state interdiffusion of cations in pellets of calcium and aluminium oxides could be influenced by establishing an electric field across the diffusing couple during heating. However, interpretation of the results was complicated both by the influence of the electric field on sintering processes within the pellets which modified their grain-boundary diffusion behaviour, and by the tendency of the CaO-Al<sub>2</sub>O<sub>3</sub> system to form a number of different product phases [1]. To remove this latter complication, the MgO-Al<sub>2</sub>O<sub>3</sub> system was chosen for study, since it forms only one product, MgAl<sub>2</sub>O<sub>4</sub> (spinel), which is also a material of practical importance in ceramics technology.

Because of its technical importance, the

reaction between MgO and Al<sub>2</sub>O<sub>3</sub> has been well studied. Carter [2] demonstrated by marker experiments on single-crystal and polycrystalline Al<sub>2</sub>O<sub>3</sub>, into which had been diffused MgO-vapour at a temperature of 1900° C in hydrogen, that a counter-diffusion of Al<sup>3+</sup> and Mg<sup>2+</sup> ions occurs across the layer of spinel reaction product. To preserve electrical neutrality, three Mg<sup>2+</sup> ions move for every two Al<sup>3+</sup> ions, leading to the formation of three molecules of spinel at the Al<sub>2</sub>O<sub>3</sub> interface for every spinel molecule formed at the MgO interface. Rossi and Fulrath [3] heated single-crystal Al<sub>2</sub>O<sub>3</sub> and MgO in air at a temperature of 1560° C for 250 h, and verified the ionic counter-diffusion mechanism. Taking account of the degree of solid solution at 1560° C, they calculated that although the spinel formed at the MgO interface should be stoichiometric, the composition of the product

formed at the  $\text{Al}_2\text{O}_3$  interface should be  $\text{Mg}_{0.63}\text{Al}_{2.24}\text{O}_4$ , from which the ratio of spinel formed at the MgO and  $\text{Al}_2\text{O}_3$  interfaces was calculated to be 1 to 4.75, in good agreement with their experimentally measured ratio of 1 to 4.83 [3]. In an electron microprobe study of the reaction of single-crystal  $\text{Al}_2\text{O}_3$  with single-crystal and polycrystalline MgO, performed in air at  $1500^\circ\text{C}$  for 70 h, Yamaguchi and Tokuda [4] measured a similar ratio of 1/4.5 of spinel formed at the MgO and  $\text{Al}_2\text{O}_3$  interfaces, respectively. Electron microprobe measurements of the Al-content of the spinel [4] indicated a smooth, continuous increase towards the  $\text{Al}_2\text{O}_3$  interface, in which region the spinel composition was  $\text{Mg}_{0.73}\text{Al}_{2.18}\text{O}_4$ , in reasonable agreement with the composition calculated by Rossi and Fulrath [3].

The aim of the present work was to investigate the effect of applied electric fields on ionic counter-diffusion in this well-understood and reasonably straightforward system. Although single-crystal studies would have avoided the complications of grain-boundary diffusion and effects such as variations in sintering, the present study was made on polycrystalline compacts because of their greater relevance to practical ceramic fabrication processes.

X-ray diffraction was used to establish product phase profiles in the reacted pellets, while elemental concentration profiles were determined by an energy-dispersive X-ray (EDAX) probe in conjunction with a scanning electron microscope. The EDAX probe was also used to determine changes in the composition of the spinel product as a function of the distance from the reaction interface and to look for compositional changes within spinel grains orientated in different directions with respect to the electric field direction.

## 2. Experimental procedure

Polycrystalline pellets of diameter 10 mm and thickness 5 mm were pressed from analytical reagent grade  $\text{Al}_2\text{O}_3$  and MgO at a pressure of  $5 \times 10^3 \text{ kg cm}^{-2}$ . The particle size of the MgO powder, estimated from scanning electron microscope (SEM) photographs, was fairly uniformly  $2 \mu\text{m}$ , whereas the alumina powder size was slightly larger, ranging from  $2 \mu\text{m} \times 5 \mu\text{m}$  to  $5 \mu\text{m} \times 10 \mu\text{m}$  chunky grains. After being separately sintered at  $1400^\circ\text{C}$  for 2.5 h in air, densification of the pellets was typically greater in the MgO than in the  $\text{Al}_2\text{O}_3$  pellets (66% and 54% of theor-

etical density respectively). MgO/ $\text{Al}_2\text{O}_3$  diffusion couples containing fine platinum wire markers were clamped between platinum foil electrodes in an electrolysis cell, described elsewhere [5], and reacted in air at temperatures in the range  $1300$  to  $1450^\circ\text{C}$  for a time of 48 h (the enhanced reactivity of the polycrystalline pellets made it possible to conduct these experiments at lower temperatures and for shorter times than those used in previous single-crystal experiments). During the diffusion anneal, direct current electric fields of typically  $4.8 \times 10^4 \text{ V m}^{-1}$  were applied across the electrodes from a Philips PW 4022 EHT power supply. Separate experiments were made with the  $\text{Al}_2\text{O}_3$  pellet negatively and positively charged, and unelectrolyzed control experiments were also made.

After quenching in air, the pellets separated easily and were cleaved in two across their diameter. One portion was used to make semi-quantitative X-ray diffraction estimates of the phase composition as a function of distance from the interface, using a grinding method described previously [1]. The other portion of the annealed couple was mounted in epoxy resin, polished on diamond laps and coated with a thin film of vacuum-deposited gold/palladium for examination using a Cambridge scanning electron microscope with an EDAX probe attachment. This method of studying changes in the Mg/Al ratio across the reaction interface was found to be preferable to electron microprobe analysis (which was also attempted) because the polycrystalline nature of the pellets made it advisable to measure mean compositional changes along the whole of the reaction boundary rather than from point to point, as with the microprobe analyzer. The EDAX measurements were made on a series of adjacent strips  $6 \mu\text{m}$  wide, and  $50 \mu\text{m}$  thick, parallel to the interface, the results being recorded as the mean Mg/Al ratio within this area. The measurements were begun immediately adjacent to the plastic filling between the two pellets and continued into the reaction zone until the measured ratio decayed to the background value, measured at the opposite edge of the pellet. Measurements were made in both the MgO and  $\text{Al}_2\text{O}_3$  pellets, in each case several traverses of various regions of each reaction zone were made, and the results were averaged to give a representative picture of the behaviour across the whole reaction area. Measurements of the excitation efficiency in pure

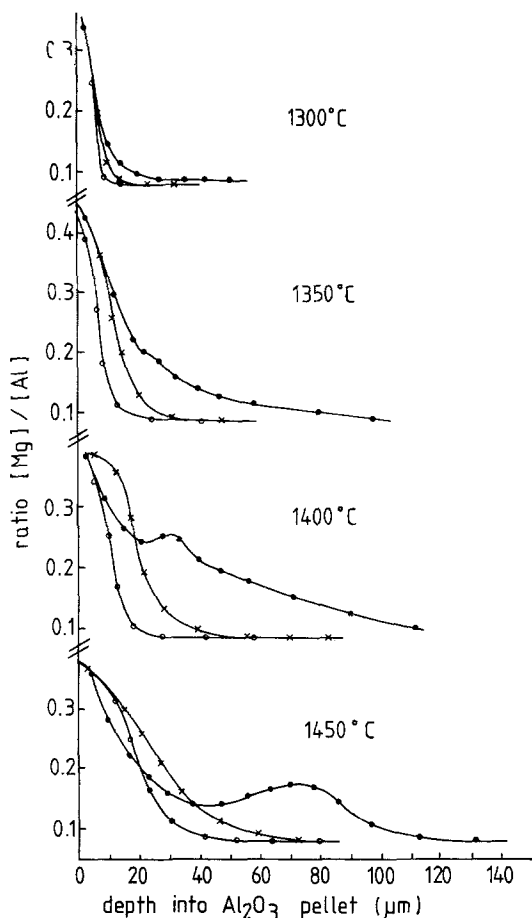


Figure 1 Diffusion profiles of Mg in electrolyzed and unelectrolyzed MgO/Al<sub>2</sub>O<sub>3</sub> couples. ● = unelectrolyzed, × = electrolyzed with alumina pellet positive, ○ = electrolyzed with alumina pellet negative. Annealing time: 48 h; mean electric field strength:  $4.93 \times 10^4 \text{ V m}^{-1}$ .

MgO and Al<sub>2</sub>O<sub>3</sub> pellets under the same experimental conditions indicated that the degree of Mg-excitation was 1.03 times that of Al; for practical purposes these were assumed to be equal.

The electrical conductances of pressed and sintered pellets of MgO and fully reacted stoichiometric MgAl<sub>2</sub>O<sub>4</sub> were measured under the same experimental conditions and temperature range as the electrolysis experiments, using a Wayne-Kerr B642 alternating current bridge operating at a frequency of 1592 Hz.

### 3. Results and discussion

#### 3.1. Elemental concentration profiles

Fig. 1 shows the behaviour of the Mg/Al ratio, measured by the EDAX probe at the four temperatures studied, as a function of depth into the Al<sub>2</sub>O<sub>3</sub> pellets.

Negligible penetration of Al into the Mg side of the couple was observed under all conditions, i.e. the ionic movement appears to be principally of Mg into Al<sub>2</sub>O<sub>3</sub> contrary to the counter-migration mechanism of spinel formation in single-crystal systems. Two points can be noted from Fig. 1:

(a) At all temperatures, the greatest penetration of Mg into Al<sub>2</sub>O<sub>3</sub> occurs when the Al<sub>2</sub>O<sub>3</sub> pellet is negatively charged;

(b) With alumina at negative polarity, a wave-front of high Mg-concentration moves into the sample at increased depth with increasing temperature (the alternative possibility that this represents a wave of Al-depletion is not consistent with the absolute values of the individual elemental count rates).

Investigation of the interfacial region by scanning electron microscopy (SEM) showed that, in the absence of an electric field, little movement of the reaction boundary with respect to the marker occurred, although in all cases there was a tendency for the marker to adhere to the MgO pellet when the couple was separated. Under conditions where the Al<sub>2</sub>O<sub>3</sub> pellet was of positive polarity, the marker adhered to the Al<sub>2</sub>O<sub>3</sub> pellet at all temperatures, whereas the reverse was the case when the polarity of the Al<sub>2</sub>O<sub>3</sub> was reversed. Although slight movement of the pellet boundaries with respect to the platinum markers was indicated, the degree of movement was small in comparison with the depth to which diffusion had proceeded, as indicated by Fig. 1. Even in the unelectrolyzed samples, the degree of penetration of Al into MgO measured by EDAX (assuming negligible boundary movement) was generally much less than the theoretically predicted ratio 1:4.75 for single crystals. A possible explanation of this is that the greater degree of sintering of the MgO pellets interferes with the diffusion of Al into that phase, whereas the more open, porous nature of the alumina pellets facilitates the entry of Mg. This suggests that the predominant diffusion mechanism is one of grain-boundary diffusion, which is quite reasonable for such polycrystalline systems. The enhanced degree of sintering of the MgO pellets was confirmed in all cases by SEM.

Fig. 1 shows that the shapes of the diffusion profiles, which were obtained under various conditions of electrolyzing field and temperature, are variable, but none of the profiles show the truly linear relationship between concentration and penetration distance predicted for grain-

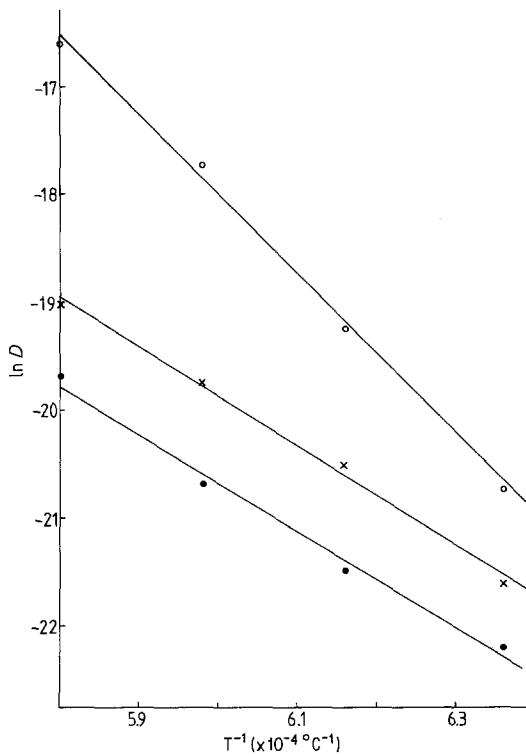


Figure 2 Temperature dependence of Mg diffusion coefficients in electrolyzed and unelectrolyzed MgO/Al<sub>2</sub>O<sub>3</sub> couples. Best-fit lines determined by regression analysis. ● = unelectrolyzed; × = electrolyzed with alumina pellet positive; ○ = electrolyzed with alumina pellet negative. Annealing time: 48 h; mean electric field strength: 5.0 × 10<sup>4</sup> V m<sup>-1</sup>.

boundary diffusion [6]. Many of the profiles are similar to that predicted for the homogeneous diffusion of a species into a semi-infinite solid with constant surface composition [6], as would apply if negligible counter-diffusion was occurring into the MgO pellet. Solution of Fick's Second Law with the appropriate boundary conditions [6] has enabled a diffusion coefficient,  $D$ , to be estimated, since

$$\frac{x}{(Dt)^{\frac{1}{2}}} = 0.954, \quad (1)$$

where  $t$  is the diffusion time and  $x$  is the point at which the concentration of the diffusing species has dropped to half its surface concentration. Plots of the temperature dependence of the diffusion coefficients calculated in this way from the observations in this work are shown in Fig. 2 for both the electrolyzed and the unelectrolyzed samples.

Linear regression analyses of Fig. 2 indicate dif-

fusion activation energies of 88.5 kcal mol<sup>-1</sup> for the unelectrolyzed samples, 91.7 kcal mol<sup>-1</sup> for samples in which the alumina is positively charged and 147.5 kcal mol<sup>-1</sup> for samples in which the alumina is negatively charged. The activation energies for the unelectrolyzed and alumina (positive) samples are of a similar magnitude to that reported for the self-diffusion of Mg in MgO (79 kcal mol<sup>-1</sup>) [7], the value of which is not very different from that reported for the diffusion of Al<sup>3+</sup> in MgO (75 kcal mol<sup>-1</sup>) [8]. The much higher activation energy of the alumina (negative) samples suggests the operation of different rate-determining processes in these samples; such a difference can also be inferred from differences in the shapes of the initial portions of the diffusion profiles, and from the presence in these samples of the concentration wave or hump already mentioned.

Over the temperature range 1300 to 1450° C, the complete expressions for the diffusion coefficients are

$$D = 4.69 \times 10^2 \exp - \left( \frac{88500}{RT} \right) \quad (2)$$

for the unelectrolyzed samples,

$$D = 2.69 \times 10^3 \exp - \left( \frac{91700}{RT} \right) \quad (3)$$

for the electrolyzed samples in which the alumina is positive, and

$$D = 3.89 \times 10^{11} \exp - \left( \frac{147500}{RT} \right) \quad (4)$$

for the electrolyzed samples in which the alumina is negative. Thus, over the present temperature range, the diffusion coefficients of Mg into Al<sub>2</sub>O<sub>3</sub> are markedly increased over the unelectrolyzed value by making the alumina side of the couple of negative polarity. By making the alumina side of the couple positive, a small increase in the diffusion coefficient is also achieved, with respect to the unelectrolyzed value.

### 3.2. Composition of the spinel phase

The results of Section 3.1 refer to the mean composition of planes in the samples parallel to the reaction interface, and provide no information about possible changes in the composition of discrete spinel grains as a function of distance into the sample, nor about possible composition

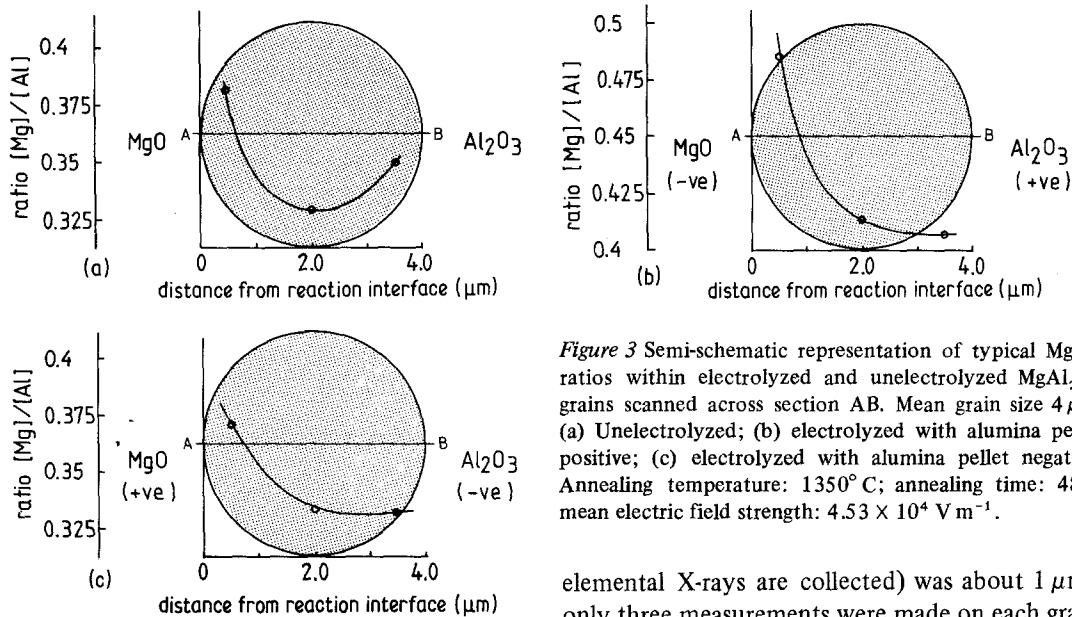


Figure 3 Semi-schematic representation of typical Mg/Al ratios within electrolyzed and unelectrolyzed  $\text{MgAl}_2\text{O}_4$  grains scanned across section AB. Mean grain size  $4\ \mu\text{m}$ . (a) Unelectrolyzed; (b) electrolyzed with alumina pellet positive; (c) electrolyzed with alumina pellet negative. Annealing temperature:  $1350^\circ\text{C}$ ; annealing time: 48 h; mean electric field strength:  $4.53 \times 10^4\ \text{V m}^{-1}$ .

changes within individual spinel grains. Point counts of the Mg/Al ratio taken within individual spinel grains at varying distances from the reaction interface gave the following results:

(a) In the unelectrolyzed control samples, the spinel composition was virtually constant over this temperature range, the mean Mg/Al ratio of 0.364 at the interface dropping only slightly to 0.347 at a distance of 8– $10\ \mu\text{m}$  into the alumina pellet.

(b) The mean Mg/Al ratio in samples in which the alumina pellet was negatively charged were similar to those of spinel in unelectrolyzed samples, but decreased more markedly with increasing distance from the interface. However, in samples in which the alumina pellet was positively charged, a considerably higher mean Mg/Al ratio was recorded in the spinel, both at the reaction interface (0.403) and at a distance of 8– $10\ \mu\text{m}$  into the alumina pellet (0.375). This is not necessarily at variance with the diffusion profiles since it could reflect a tendency to form fewer spinel particles of higher Mg-content under these conditions.

Typical results of composition determinations within some of the larger discrete spinel grains are shown semi-schematically in Fig. 3. For the purpose of these measurements, grains of approximately similar size and morphology were selected and their compositions probed along an axis normal to the reaction interface. Since, under the present instrumental operating conditions the effective probe size (the volume from which the

elemental X-rays are collected) was about  $1\ \mu\text{m}^3$ , only three measurements were made on each grain, one at each edge and one near the centre. In the unelectrolyzed control sample, the highest Mg-concentrations were recorded at the outer edges of the grains in all cases, consistent with the formation of spinel by diffusion of Mg into an alumina grain (Fig. 3a). Furthermore, little asymmetry was noted between the sides of the grains closest to the MgO source and those furthest away, suggesting that the reacting MgO has completely surrounded the  $\text{Al}_2\text{O}_3$  grains, possibly by vapour-phase transport through the alumina pore structure. By contrast, in electrolyzed samples of both positive and negative alumina polarity, considerably higher Mg concentrations were recorded in the grain regions closest to the MgO source (Fig. 3b and c). In the samples in which the alumina was positively charged, particularly high Mg-concentrations were recorded nearest the interface (Fig. 3b), confirming the result (b) above in this section.

At least three possible explanations exist for these results. If the MgO is assumed to enter the porous alumina structure in the vapour phase, the higher concentrations of Mg occurring in the spinel grains when the alumina pellet is positively charged could imply a negatively-charged vapour species. This does not seem very likely. A second possibility is that oxide ion migration plays an essential role in the formation of the spinel interface, but this also appears unlikely for the unelectrolyzed samples and is probably also so in the electrolyzed samples, in view of an  $^{18}\text{O}$ -tracer study by Nakano *et al.* [9] in which the mechanism of spinel formation was clearly shown to

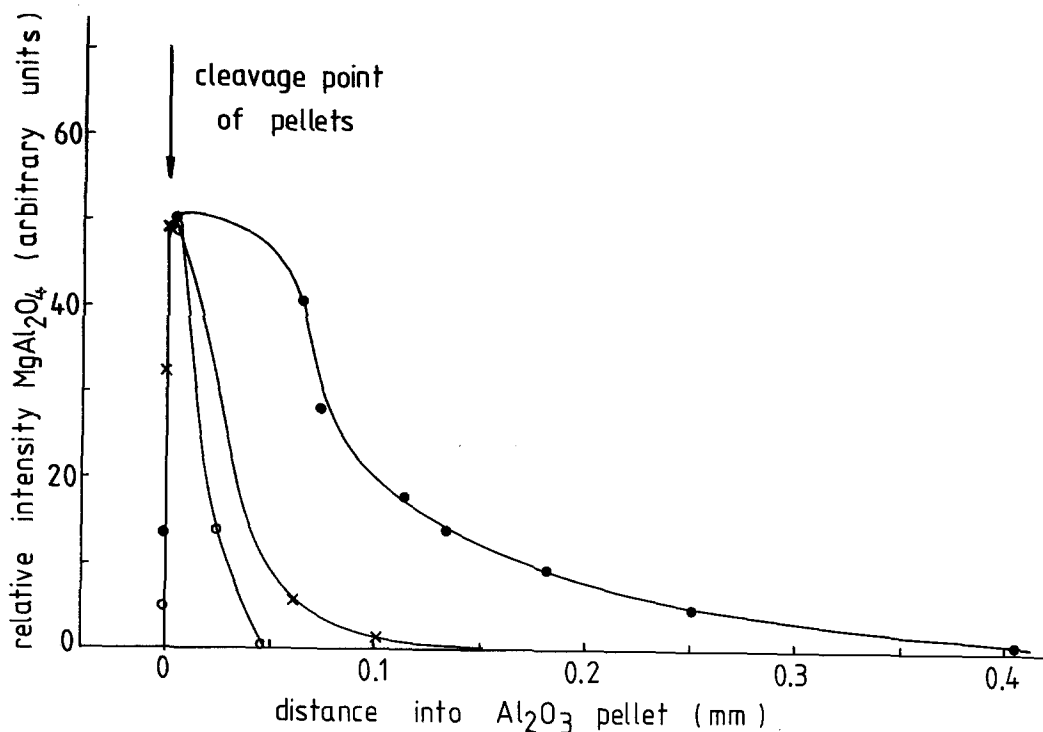


Figure 4 Typical  $\text{MgAl}_2\text{O}_4$  profiles determined by X-ray diffraction in electrolyzed and unelectrolyzed  $\text{MgO}/\text{Al}_2\text{O}_3$  couples. Annealing temperature:  $1400^\circ\text{C}$ ; annealing time: 48 h; mean electric field strength:  $4.51 \times 10^4 \text{ V m}^{-1}$ . ● = unelectrolyzed; × = electrolyzed with alumina pellet positive; ○ = electrolyzed with alumina pellet negative.

involve the movement of cations through an immobile oxygen lattice. A third alternative is that with the alumina at positive polarity, a counter-migration of the smaller Al-ions is established from the alumina-rich side furthest away from the interface to the spinel reaction layer, in the direction of the negatively-charged MgO pellet. This would explain a build-up of Al in the spinel grains at the side furthest away from the interface, but could only account for the abnormally high Mg-content in the region of grains nearest the interface if Al is assumed to continue migrating out of the grain and towards the interface. The data of Roy *et al.* [10] on the solid solubility of spinel in  $\text{Al}_2\text{O}_3$  indicate that 43.5 mol% MgO can exist in spinel at an alumina boundary at  $1300^\circ\text{C}$ ; this value decreases to 39.8 mol% MgO at  $1450^\circ\text{C}$ . These values correspond to Mg/Al ratios of 0.385 and 0.331 at 1300 and  $1450^\circ\text{C}$ , respectively. Thus, the spinel compositions of the unelectrolyzed samples are very close to the compositions predicted from the solid solubility data [10], but those of the electrolyzed grains are rather too high in Mg, especially in the alumina (positive) samples. This raises the question whether the outer regions of such grains are indeed spinel; X-ray diffraction

(see below) indicates the presence of MgO in the alumina component of the electrolyzed couples.

### 3.3. X-ray phase profiles in the reacted pellets

Fig. 4 shows typical concentration profiles of the spinel phase, determined semi-quantitatively by X-ray diffraction, as a function of penetration depth into the  $\text{Al}_2\text{O}_3$  pellet.

Since the pellets did not bond together during heating, the point of reference for the depth measurements was taken as the point of cleavage. No significant spinel formation was detected in any of the MgO pellets, apart from a light, dusty surface-coating at the interface which could be readily wiped off. Fig. 4 confirms the EDAX probe results that the greatest depth of Mg-penetration into  $\text{Al}_2\text{O}_3$  occurred when the alumina pellet was negatively charged. A slight enhancement in the depth of product formation was also observed under conditions of reversed polarity, again suggesting that a counter-migration of Al was occurring (albeit to a limited extent, as indicated by the marker experiments).

The shapes of the spinel distribution curves (Fig. 4) are different from those of the Mg/Al

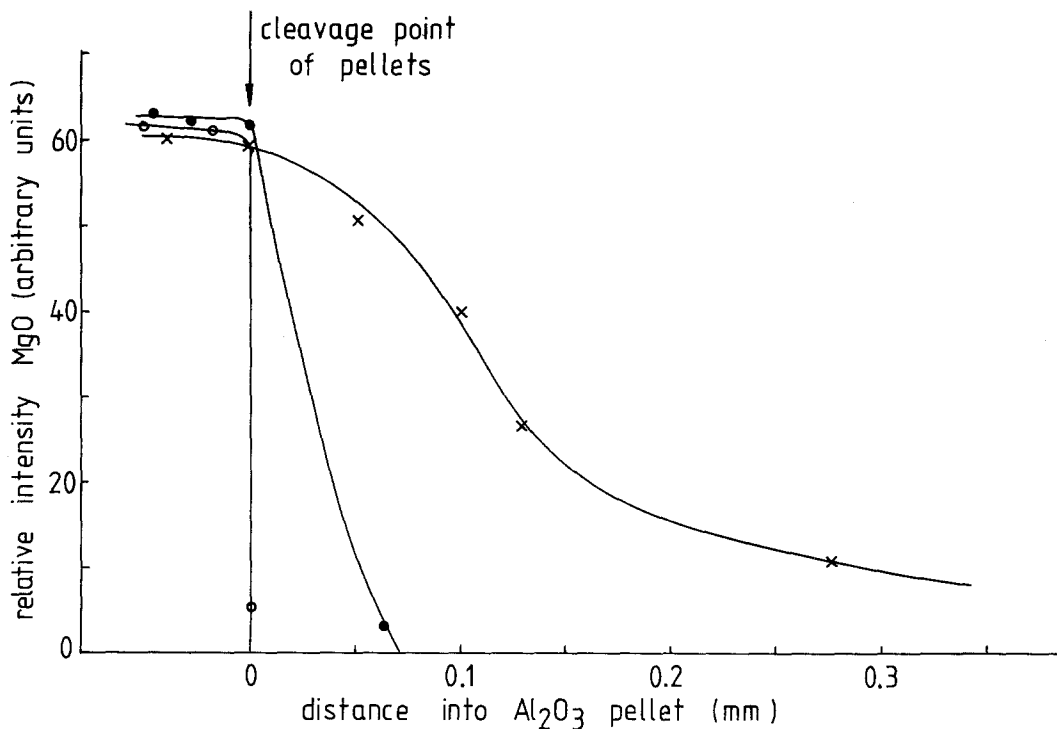


Figure 5 Typical MgO profiles within the alumina pellets of electrolyzed and unelectrolyzed MgO/Al<sub>2</sub>O<sub>3</sub> couples, determined by X-ray diffraction. Annealing temperature: 1400° C; annealing time: 48 h; mean electric field strength:  $4.51 \times 10^4 \text{ V m}^{-1}$ . ● = unelectrolyzed; × = electrolyzed with alumina pellet positive; ○ = electrolyzed with alumina pellet negative.

profiles, particularly in the region close to the interface. There are two possible reasons for this:

(a) the X-ray determination does not take account of the considerable variation in spinel stoichiometry which has been shown by EDAX probe results to occur throughout the reaction layer;

(b) X-ray diffraction analysis shows that, in addition to spinel formation, Mg also occurs as MgO in the Al<sub>2</sub>O<sub>3</sub> component of electrolyzed couples.

A typical MgO-phase profile is shown in Fig. 5, indicating the presence of MgO at considerable depth in the alumina (positive) pellets and at less depth in the alumina (negative) pellets. No MgO was detected in the alumina component of the unelectrolyzed couples.

An extensive SEM/EDAX search of the electrolyzed samples failed to locate any discrete MgO grains within the reaction layers and it was concluded that this oxide occurs in a thin layer on the spinel grains which would not be resolved by the EDAX probe (indicating a layer thickness less than the effective probe diameter of  $\sim 1 \mu\text{m}$ ). In this way the unexpectedly high Mg-concentrations

recorded at the interface edges of the spinel grains, particularly in the alumina (positive) samples, could be explained.

An interesting implication of these curious results is that transport of Mg (or MgO) into the alumina is enhanced by electrolysis, irrespective of the polarity of the pellets, but the depth of penetration is greatest where the alumina is negatively charged, as would be expected if the migrating species was Mg<sup>2+</sup>. Under alumina (negative) conditions, the penetration of Mg to greater depth ensures that the system remains more or less within the stability range for spinel at that temperature, except in the region immediately adjacent to the interface, where the excess MgO precipitates in a thin layer on the spinel grains upon cooling. Under alumina (positive) conditions, the transport of excess Mg or MgO within the pore structure of the alumina is again enhanced but its penetration distance is reduced. The resulting high local concentrations of Mg cause the spinel stability field to be more extensively exceeded and lead to the precipitation of MgO on the spinel grain surfaces at a greater depth within the alumina pellet. One unexplained

aspect of the results is the mechanism by which the transport of MgO (possibly in the vapour phase) appears to be influenced by electric fields. No explanation is presently available for this observation.

### 3.4. Effective electrical mobility of the migrating species

The down-field shift of the diffusion profile,  $\Delta$ , is related to the effective electrical mobility of the migrating species,  $\mu_{\text{eff}}$ , the diffusion time,  $t$ , and the applied field strength,  $E$ , by

$$\Delta = \mu_{\text{eff}} Et. \quad (5)$$

Studies of the CaO–Al<sub>2</sub>O<sub>3</sub> system [1] have suggested that a reasonable prediction of the down-field shift can be made using a value of  $\mu_{\text{eff}}$  calculated from

$$\mu_{\text{eff}} \approx \mu(\sigma_0/\sigma), \quad (6)$$

where  $\mu$  is the true electrical mobility of the migrating species (as measured in the pure oxide), and  $\sigma_0$  and  $\sigma$  are the electrical conductivities of the pure oxide and product phase (in this case, spinel), respectively. As a further test of the applicability of these relationships, the effective electrical mobilities derived from the down-field shifts measured in this work were compared with effective mobilities calculated from Equation 6. Values for the electrical conductivities of the polycrystalline spinel phase were determined over this temperature range in a separate set of experiments.\* Since the electrical conductance of polycrystalline compacts is influenced by the grain size and the thermal history of the sample, the spinel samples were synthesized from the same oxides and reacted over a similar temperature range as those employed in the electrolysis experiments. For consistency, the conductivities of sintered MgO pellets were also determined under identical conditions (Fig. 6). Linear regression analysis of the data of Fig. 6 resulted in the expression

$$\sigma = 7.42 \times 10^2 \exp \left( -\frac{41\,700}{RT} \right) \quad (7)$$

for the conductance of spinel over the temperature range 1100–1550°C while the conductance of MgO over the temperature range 1300–1580°C

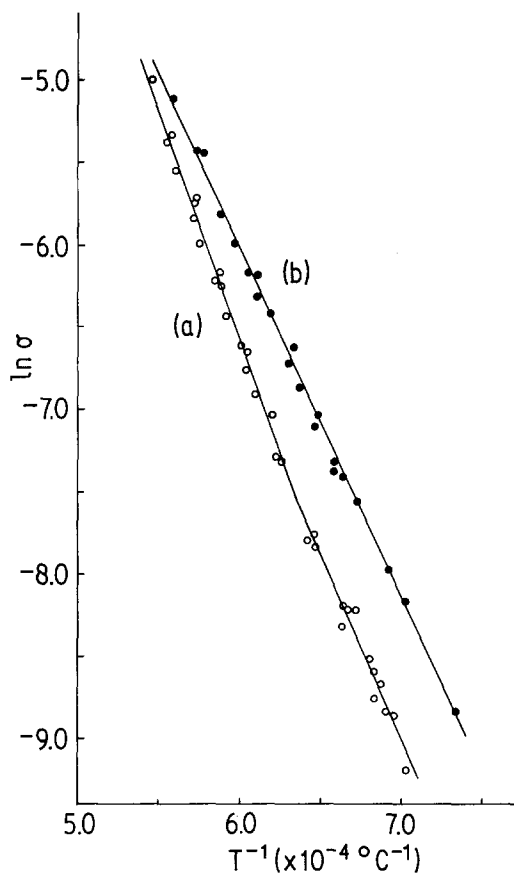


Figure 6 Temperature dependence of electrical conductance of MgO and MgAl<sub>2</sub>O<sub>4</sub> polycrystalline pellets in air. Best fit lines determined by regression analysis. (a) MgO, results from four experiments. (b) MgAl<sub>2</sub>O<sub>4</sub>, results from three experiments.

could be expressed as

$$\sigma = 2.34 \times 10^4 \exp \left( -\frac{54\,900}{RT} \right). \quad (8)$$

The electrical mobility of Mg in MgO,  $\mu$ , was calculated from the Nernst–Einstein equation

$$\mu = Dze/kT, \quad (9)$$

where  $z$  is the valancy of the migrating species,  $e$  is the electronic charge,  $D$  is the self-diffusion coefficient of Mg in MgO, taken from the data of Lindner and Parfitt [7],  $k$  is the Boltzmann constant and  $T$  is the temperature.

Values of  $\mu_{\text{eff}}$  thus calculated from Equation 6 are shown in Table I, together with values derived

\*Since the preparation of this manuscript, a conductance study of pure, single-crystal MgAl<sub>2</sub>O<sub>4</sub> has appeared [11] indicating an activation energy for the temperature range of interest here of 49.8 kcal mol<sup>-1</sup>, which is a value in reasonable agreement with the present value for polycrystalline samples. For the purposes of this calculation, however, the polycrystalline conductances are preferred, since they relate more closely to the system under investigation.



TABLE I Effective electrical mobilities of Mg in MgAl<sub>2</sub>O<sub>4</sub> estimated from diffusional shift distances, Δ, and calculated from conductance data by Equation 6. Diffusion time  $t = 1.728 \times 10^5$  sec; mean field strength  $E = 4.93 \times 10^2$  V cm<sup>-1</sup>

Temperature (° C)	Δ (× 10 <sup>-2</sup> cm)	μ <sub>eff</sub> (from Equation 5) (× 10 <sup>-10</sup> cm <sup>2</sup> sec <sup>-1</sup> V <sup>-1</sup> )	σ <sub>o</sub> /σ	μ <sub>eff</sub> (from Equation 6) (× 10 <sup>-10</sup> cm <sup>2</sup> sec <sup>-1</sup> V <sup>-1</sup> )
1300	0.65	0.76	0.47	0.18
1350	1.8	2.1	0.52	0.41
1400	4.4	4.2	0.58	0.93
1450	7.7	9.1	0.66	2.1

from the down-field shifts estimated from the diffusion profiles of Fig. 1. Table I shows that the agreement between the calculated and measured effective mobilities is reasonable, bearing in mind the approximate nature of Equation 6 and the difficulty of measuring down-field shifts from diffusion profiles the shapes of which may have been altered by electrolysis. Interestingly, the effective mobilities calculated from the conductance data are consistently lower than the values derived from the measured down-field shifts by a factor of about 4.5; a similar result was recorded in a previous study of the CaO–Al<sub>2</sub>O<sub>3</sub> system [1] where μ<sub>eff</sub> derived from conductance measurements was about ~ 4.2 times smaller than μ<sub>eff</sub> derived from the down-field shift. The significance of this result is not understood at present, but it may be related to ion–ion or ion–vacancy pairing in these divalent–trivalent systems which is not taken into account in Equation 6. Under these circumstances, Equations 5 and 6 should probably be regarded as only a guide to the diffusional behaviour of mixed-valency oxide systems under the influence of electric fields, especially where counter-migration and second-phase formation becomes significant.

#### 4. Conclusions

(a) Diffusion in polycrystalline MgO–Al<sub>2</sub>O<sub>3</sub> couples is enhanced by applying external direct current electric fields, especially when the alumina pellet is negatively charged. In the present samples, both for these samples electrolyzed and unelectrolyzed, the principal migration is of Mg into Al<sub>2</sub>O<sub>3</sub> rather than vice-versa, possibly as a result of a higher degree of sintering in the MgO pellets which interferes with grain-boundary diffusion in that phase. Electrolysis increases the values of the diffusion coefficients, as estimated from the MgO concentration profiles in the Al<sub>2</sub>O<sub>3</sub> pellets, especially where the alumina pellet is of negative polarity. The activation energy for diffusion is

similar in the unelectrolyzed control samples to the case where the alumina pellet is positively charged (88–92 kcal mol<sup>-1</sup>) but is increased to 147 kcal mol<sup>-1</sup> where the alumina pellet is of negative polarity.

(b) The spinel phase formed at the interface between the two pellets extends principally into the alumina pellet. In the unelectrolyzed samples its composition corresponds well with that calculated from solid solubility data, but in the electrolyzed samples the Mg-content is higher than predicted, especially in the alumina (positive) samples. The excess Mg apparently resides in the surface regions of the spinel grains, especially at the sides of the grains nearest to the pellet interface, where it precipitates as a surface layer of MgO.

(c) Calculations of the effective electrical mobility of Mg<sup>2+</sup> in this system, derived from electrical conductivity measurements, compare only moderately well with values derived from the measured down-field shifts of the diffusion profiles. This discrepancy is due both to difficulties in the down-field shift measurements and to the approximate nature of the calculation involving the conductivity measurements.

#### Acknowledgement

We are indebted to Mr G. D. Walker for the SEM/EDAX measurements.

#### References

1. K. J. D. MACKENZIE and R. K. BANERJEE, *J. Mater. Sci.* **14** (1979) 339.
2. R. E. CARTER, *J. Amer. Ceram. Soc.* **44** (1961) 116.
3. R. C. ROSSI and R. M. FULRATH, *ibid.* **46** (1963) 145.
4. G. YAMAGUCHI and T. TOKUDA, *Bull. Chem. Soc. Japan* **40** (1967) 843.
5. K. J. D. MACKENZIE, *Trans. J. Brit. Ceram. Soc.* **77** (1978) 13.
6. P. KOSTAD, "Nonstoichiometry, Diffusion and Electrical Conductivity in Binary Metal Oxides"

- (Wiley Interscience, New York, 1972) p. 70.
7. R. LINDNER and G. D. PARFITT, *J. Chem. Phys.* **26** (1957) 182.
  8. V. S. STUBICAN, C. GRESKOVICH and W. P. WHITNEY, *Mater. Sci. Res.* **6** (1972) 55.
  9. M. NAKANO, G. YAMAGUCHI and K. SAITO, *Yogyo Kyokai Shi*, **79** (1971) 92.
  10. D. M. ROY, R. ROY and E. F. OSBORN, *Amer. J. Sci.* **251** (1953) 337.
  11. R. A. WEEKS and E. SONDER, *J. Amer. Ceram. Soc.* **63** (1980) 92.

Received 29 May and accepted 10 July 1980.